Separation Science and Technology
Publication details, including instructions for authors and subscription information:
http://www.informaworld.com/smpp/title~content=t713708471

# Effect of Polymer Membrane Material on Reverse Osmosis Separations of Free Radicals in Aqueous Solutions

Kam Chan[a]; Takeshi Matsuura[a]; S. Sourirajan[a]
[a] DIVISION OF CHEMISTRY, NATIONAL RESEARCH COUNCIL OF CANADA, OTTAWA, ONTARIO, CANADA

**To cite this Article** Chan, Kam , Matsuura, Takeshi and Sourirajan, S.(1983) 'Effect of Polymer Membrane Material on Reverse Osmosis Separations of Free Radicals in Aqueous Solutions', Separation Science and Technology, 18: 9, 843 — 855

**To link to this Article: DOI:** 10.1080/01496398308060309

**URL:** http://dx.doi.org/10.1080/01496398308060309

SEPARATION SCIENCE AND TECHNOLOGY, 18(9), pp. 843-855, 1983

# Effect of Polymer Membrane Material on Reverse Osmosis Separations of Free Radicals in Aqueous Solutions

---

KAM CHAN, TAKESHI MATSUURA, and S. SOURIRAJAN

DIVISION OF CHEMISTRY
NATIONAL RESEARCH COUNCIL OF CANADA
OTTAWA, ONTARIO, CANADA K1A 0R9

## Abstract

The reverse osmosis separations of four different piperidinooxy free radicals, one undissociated piperidine solute, and one dissociated hydrochloride solute of similar molecular structure were studied by using cellulose acetate (CA-398) and aromatic polyamidohydrazide (PPPH 8273) membranes of different surface porosities under different operating pressures. Liquid chromatography experiments were conducted parallel to the reverse osmosis experiments, and the order of the preferential sorption among solute compounds and solvent water was found to be, ionic solutes $<$ $D_2O$ $<$ radical solutes $<$ nonionized solute in the case of cellulose acetate material, and ionic solutes $<$ radical solutes $<$ $D_2O$ $<$ nonionized solute in the case of aromatic polyamidohydrazide, with the one exception of the piperidinooxy free radical containing an amino group which was slightly more strongly adsorbed to the latter polymeric material than $D_2O$. The above order of preferential adsorption is reflected in the reverse osmosis separation data. The surface force–capillary flow model was also applied to predict the reverse osmosis performance data. The method is illustrated and results are discussed.

## INTRODUCTION

Stable free nitroxyl radicals have been widely studied in the field of organic chemistry and biochemistry; they have recently been used for the stabilization of polymers (*1*). Since the membrane separation of these radicals is of biomedical significance (*2*), their reverse osmosis (RO) separations were studied by using cellulose acetate membranes, and the results were reported in a previous paper (*3*). Liquid chromatography (LC)

0149-6395/84/1809-0843$3.50/0

experiments were also carried out with respect to cellulose acetate–water–free radicals systems parallel to RO experiments, and the following results were obtained.

(1) Both radicals are positively separated by reverse osmosis using cellulose acetate membranes.

(2) The preferential sorptions of piperidinooxy radicals at a cellulose acetate material–aqueous solution interface lie intermediate between those of undissociated piperidine solute and dissociated hydrochloride solutes of structurally similar compounds, and are closer to those of the latter compounds.

(3) The order of the preferential sorption of the solute to cellulose acetate polymer is reflected in the order of the reverse osmosis separation and especially in the pressure effect on the latter order.

In this paper, as an extension of a previous report, we have further studied the reverse osmosis separations of four different nitroxyl radicals as well as one undissociated piperidine solute and one dissociated hydrochloride solute of similar molecular structure using cellulose acetate (CA-398) and aromatic polyamidohydrazide (PPPH 8273) membranes of different porosities under different operating pressures. Despite the different variables involved in this study, the change in the preferential adsorption characteristics of free radical solutes on different polymer materials and its effect on the membrane separation of the above solutes is the central theme of this paper. Furthermore, the transport equations developed on the basis of the surface force–pore flow model are applied to the reverse osmosis performance data and the predictive capability of the transport equations is examined.

The method used and the results obtained are illustrated.

## EXPERIMENTAL

### Liquid Chromatography (LC) Experiments

A liquid chromatograph model ALC 202 of Waters Associates fitted with a different refractometer was used in this work. The method of column preparation and the general experimental technique used were the same as those reported earlier (*4*). Briefly, solutes were injected into the solvent water stream which flows through a column packed with membrane polymer powder. The particle size was kept in the range 38–53 μm by sieving and the column length was 60 cm. The solvent flow rate through the column was fixed at 0.275 $cm^3$/min. Ten μL of sample solution (1 wt% solute) was injected into the column and the retention volume was determined. In the case of heavy water, 10 wt% solution was used as the sample.

## Reverse Osmosis Membranes

Cellulose acetate Eastman E-398 (CA-398) membranes of different surface porosities made in the laboratory by the method described earlier (5), were used. In this method the average pore size on the membrane surface was controlled by changing the shrinkage temperature. Aromatic polyamidohydrazide (PPPH 8273) membranes of different surface porosities were also made in the laboratory by the method described earlier (*6*), in which the porosity of the membrane was controlled by changing the evaporation time of the solvent.

## Reverse Osmosis Experiments

Each membrane was subjected to an initial pure water pressure of 11,721 kPa gauge (= 1,700 psig) for about 2 h prior to subsequent use in reverse osmosis experiments, all of which were carried out in the operating pressure range of 1,724 to 10,342 kPa gauge (= 250 to 1,500 psig) and at laboratory temperature (23–25°C). For the purpose of membrane specifications in terms of pure water permeability constant $A$ (in kg · mol of $H_2O/m^2 \cdot s \cdot kPa$) and solute transport parameter $(D_{AM}/K\delta)$ (treated as a single quantity, m/s), aqueous feed solutions containing 3500 ppm of NaCl were used (*7*). Data on $A$ and $(D_{AM}/K\delta)$ so obtained are listed in Table 1 with respect to all membranes used in this work together with experimental reverse osmosis data of sodium chloride solute. In all other experiments the solute concentrations in the aqueous feed solutions were so low (0.001 molal) that the osmotic pressures involved were negligible compared to the operating pressure. In each experiment, the fraction solute separation, defined as

$$f = \frac{\text{solute ppm in feed} - \text{solute ppm in product}}{\text{solute ppm in feed}}$$

TABLE 1

Film Specification[a]

| Film number | CA-1 | CA-2 | PPPH 8273-1 | PPPH 8273-2 |
|---|---|---|---|---|
| Operating pressure, 10,342 kPag (1,500 psig). Pure water permeability constant, | | | | |
| $A, \left(\frac{\text{kg}\cdot\text{mol H}_2\text{O}}{\text{m}^2\cdot\text{s}\cdot\text{kPa}}\right) \times 10^7$ | 0.416 | 0.642 | 0.330 | 0.367 |
| Solute transport parameter $(D_{AM}/K\delta)_{NaCl}$, m/s × $10^7$ | 5.04 | 16.10 | 0.634 | 3.63 |
| Mass transfer coefficient,[b] $k_{NaCl}$, m/s × $10^6$ | 24.00 | 22.70 | 20.63 | 20.89 |
| Sodium chloride data. | | | | |
| Solute separation, % | 91.0 | 81.2 | 98.6 | 93.0 |
| Product rate, kg/h × $10^3$ [c] | 38.0 | 58.5 | 30.1 | 33.5 |
| Glycerol data. | | | | |
| Solute separation, % | 76.5 | 66.5 | 95.2 | 90.0 |
| Product rate, kg/h × $10^3$ [c] | 41.00 | 64.68 | 31.20 | 33.64 |
| Pore diameter, $2R_b$, × $10^{10}$m | 8.70 | 9.11 | 4.74 | 6.12 |

[a] Concentration of feed solution; sodium chloride, 0.06 molal; glycerol, 0.002 molal.

[b] Feed flow rate, 400 × $10^{-6}$ $m^3$/min.

[c] Area of film surface, 13.2 × $10^{-4}$ $m^2$.

membrane permeated product rate (PR), and pure water permeation rate (PWP) in kg/h for the effective area of membrane surface used (= 13.2 $cm^2$ in this work) were determined at the specified operating conditions. All reverse osmosis experiments were for single solute systems. The following organic solutes were used in this study.

I. 2,2,6,6-Tetramethyl-4-piperidone hydrochloride

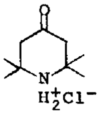

II. 4-Hydroxy-2,2,6,6-tetramethyl piperidine hydrochloride

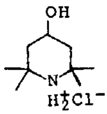

III. 2,2,6,6-Tetramethyl piperiodinooxy free radical

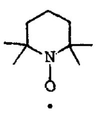

IV. 4-Oxo-2,2,6,6-tetramethyl piperidinooxy free radical

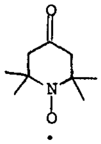

V. 4-Hydroxy-2,2,6,6-tetramethyl piperidinooxy
free radical

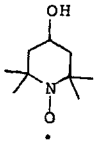

VI. 4-Amino-2,2,6,6-tetramethyl piperidinooxy
free radical

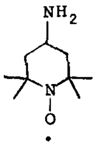

VII. 4-Hydroxy-2,2,6,6-tetramethyl piperidine

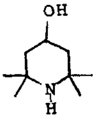

All of the above reagents were recrystallized in methanol prior to use in RO experiments.

A total carbon analyzer (Beckman model 915A) was used to determine the concentration of the organic solutes in feed and membrane permeated product solutions, and the stability of the free radicals during membrane permeation was confirmed by their detection in the product solution by electron spin resonance. The concentrations of sodium chloride were determined using a conductivity bridge.

## RESULTS AND DISCUSSION

### Liquid Chromatography Data

The data on the retention volume and the specific surface excess for each solute studied with respect to CA-398 and PPPH 8273 polymers are listed in Table 2. The specific surface excess data for solute A, $\Gamma_A/c_b$, was calculated by (*8*)

$$\Gamma_A/c_b = \frac{[V'_R]_A - [V'_R]_{\text{water}}}{A_p} \tag{1}$$

where $\Gamma_A$, $c_b$, $[V'_R]_A$, $[V'_R]_{\text{water}}$, and $A_p$ denote surface excess of the solute A, the concentration of the solute in the bulk solution, the retention volume of solute A, the retention volume of water represented by that of heavy water, and the total surface area $A_p$ of the polymer powder in the column, respectively. The quantity $A_p$ was determined by the GC method or by the adsorption of *p*-nitrophenol described in an earlier paper (*9*). The values of $A_p$ used in this work are reported in Table 2.

With respect to CA-398 material, the increasing order of the retention volume is ionic solutes (I, II) < $D_2O$ < radical solutes (III, IV, V, VI) << nonionized solute (VII). These data indicate that ionic solutes are rejected, radicals are weakly attracted, and nonionized solute (VII) is strongly

TABLE 2
Some Chromatographic Data and Surface Properties of Polymer Materials[a]

| Solute number | CA-398 polymer: Retention volume (cm$^3$) | CA-398 polymer: $\Gamma/c_b \times 10^{10}$ (m) | PPPH 8273 polymer: Retention volume (cm$^3$) | PPPH 8273 polymer: $\Gamma/c_b \times 10^{10}$ (m) |
|---|---|---|---|---|
| I | 2.05 | −7.6 | 3.67 | −5.7 |
| II | 2.05 | −7.6 | 3.60 | −6.8 |
| III | 3.00 | 6.4 | 3.70 | −5.1 |
| IV | 3.91 | 19.7 | 3.80 | −3.4 |
| V | 3.00 | 6.4 | 3.70 | −5.1 |
| VI | 4.07 | 22.0 | 4.45 | 7.7 |
| VII | 24.00 | 314.5 | 8.83 | 82.1 |

[a] Retention volumes of $D_2O$; for CA-398 polymer 2.57 cm$^3$, for PPPH 8273 polymer 4.00 cm$^3$. $A_p$ used in Eq (1): for CA-398 polymer 684 m$^2$, for PPPH 8273 polymer 579 m$^2$.

attracted to the polymer material at the polymer–solution interface; these results are consistent with those reported in our previous work (*3*).

With respect to PPPH 8273 polymer material, the increasing order of the retention volume is ionic solutes (I, II) ≈ radical solutes (III, IV, V) < $D_2O$ < radical solute (VI) < nonionized solute (VII). A remarkable change took place in the positions of free radical solutes (III, IV, V), which are now located before $D_2O$, indicating the rejective force on these solutes from the polymer surface. The relative positions of other solutes remained unchanged. The stronger rejection on the radicals (III, IV, V) from aromatic polyamidohyrazide material may be due to the stronger repulsive forces exerted from amide —CO—NH— of the polyamidohydrazide; the 4-amino-2,2,6,6-tetramethyl piperidinooxy free radical (VI) is, however, slightly adsorbed by polyamidohydrazide owing to the hydrogen bonding capability of the amino group in the radical. Considering the basic property of cellulose acetate material (*10*) and the acidic property of aromatic polyamidohydrazide material (*11, 12*), the above data on chromatographic retention volumes are consistent with the acidic nature of the piperidinooxy radicals.

Since the backbone nitroxyl structure is identical for all solute molecules under study, the steric hindrance (restriction on the movement of the solute molecule in the pore) must be nearly equal for all the solutes involved. Hence, any difference in the solute separation in reverse osmosis must be attributed to the difference in the interaction forces such as those demonstrated in the retention volume data of LC experiments. For example, the order in the reverse osmosis separation of the solute by CA-398-1 membrane at the operating pressure of 10,342 kPag (1,500 psig) is ionic solute (I, 93.8%) > radical solutes (III, 86.7%; IV, 85.7%; V, 88.0%; VI, 88.8%) > nonionized solute (VIII, 85.4%). Likewise, the reverse osmosis data with respect to PPPH 8273-2 membrane at the operating pressure of 10,342 kPag (1,500 psig) shows the order of solute separation as ionic solute (I, 95.0%) ≈ radical solutes (III, 96.9%; IV, 95.7%; V, 96.0%) > radical solute (VI, 89.3%) > nonionized solute (VII, 77.1%). These orders are precisely the same as the decreasing order of the rejective force (or the increasing order of the attractive force) working between the solute and the membrane material. Although the order in the reverse osmosis separation might change slightly from the ones presented above, depending on the pore structure and the operating pressure, the general pattern in the correspondence between LC and RO data is unaltered.

## Predictability of the Reverse Osmosis Separation Data

The transport equations used for the determination of the interaction force constant, average pore radius, and for the prediction of the membrane performance data have been reported in detail in our earlier work and, therefore, are not repeated. These transport equations are based on the surface force-pore flow model (*13, 14*) in which the following assumptions are made:

(1) The transport of the solvent and the solute takes place through cylindrical pores of radius $R_b$ running across the active skin layer perpendicular to the membrane surface.

(2) The solvent phase is continuous. Its radial velocity profile can be given by solving the momentum balance equation, considering all forces working on the solvent fluid. In the absence of the solute, the velocity profile is the same as that of Poiseuille flow.

(3) The radial concentration profile of the solute in the cylindrical pore is given by applying the Maxwell-Boltzmann equation to the interaction potential profile defined as the function of the distance from the pore wall. As such interaction potential functions,

$$\phi_{\text{electrostatic}} = \begin{cases} \infty & \text{for } d \leq \mathbf{D} \\ \dfrac{\mathbf{A}}{d}(\mathbf{R}T) & \text{for } d > \mathbf{D} \end{cases} \tag{2}$$

and

$$\phi_{\text{van der Waals}} = \begin{cases} \infty & \text{for } d \geq \mathbf{D} \\ -\dfrac{\mathbf{B}}{\alpha^3}(\mathbf{R}T) & \text{for } d > \mathbf{D} \end{cases} \tag{3}$$

are used for electrostatic and van der Waals interaction forces, respectively (*13*), where $\phi$, **A**, **B**, **D**, and $d$ denote the potential due to the interaction force, the force constant representing the electrostatic force, that representing the van der Waals force, that representing the steric hindrance, and the distance between the center of the solute and the polymer–solution interface, respectively. The quantities **R** and $T$ are gas constant and absolute temperature, respectively.

(4) A stronger frictional force than in bulk water is working on the solute in the membrane pore, which restricts the movement of the latter species. The ratio of such a frictional force to that in the bulk water, $b$, was given empirically (*14*) by

$$b = \begin{cases} 1/(1 - 2.104\lambda + 2.09\lambda^3 - 0.95\lambda^5), & \lambda \le 0.22 \\ 44.57 - 416.2\lambda + 934.9\lambda^2 + 302.4\lambda^3, & 1 > \lambda > 0.22 \end{cases} \tag{4}$$

where $\lambda = \mathbf{D}/R_b$.

(5) The concentration polarization in the vicinity of the membrane surface is taken into consideration.

The transport equations so developed establish a unique relationship among three quantities **A** (or **B**), **D**, $R_b$, and the reverse osmosis solute separation $f$ under a given set of operating conditions. On the other hand, the specific surface excess $\Gamma/c_b$ obtained from the LC data is related to the interfacial potential functions such as Eqs. (2) and (3) by

$$\Gamma/c_b = \int_{\mathbf{D}_{\text{water}}}^{\infty} (e^{-\phi/\mathrm{R}T} - 1)d(d) \tag{5}$$

where $\mathbf{D}_{\text{water}}$ is the molecular radius of water (*14*). By Eq. (5) a unique relationship is established among quantities $\Gamma/c_b$, **A** (or **B**), and **D**. Consequently, five quantities, $f$, $\Gamma/c_b$, **A** (or **B**), **D**, and $R_b$, are under the restriction of two unique relations, one the transport equations and the other Eq. (5) for the surface excess. Considering the first two quantities are obtainable by experiment, the last three unknowns can be determined if one of the three quantities is given *a priori*. This is the principle of determining the force constants **A** (or **B**), **D**, and the pore radius $R_b$. The procedure of the determination is as follows.

In the first step glycerol is chosen as a reference solute and RO and LC experiments are carried out. Thus, we obtain $f$ and $\Gamma/c_b$ of glycerol. Then, the quantity **D** is equated to the Stokes' law radius of glycerol solute ($2.3 \times 10^{-10}$ m). Applying the above principle, the force constant **B** (**A** is nonexistent since there is no electrostatic repulsive force working between glycerol solute and the polymer surface) and the pore radius $R_b$ for the particular membrane used for the RO experiment are calculated. This procedure is employed for each membrane used in the study and the resulting $R_b$ values are listed in Table 1 together with the glycerol separation data.

In the second step both RO and LC experiments are conducted with respect to each solute listed in Table 2, thus data on $f$ and $\Gamma/c_b$ become available for each solute under study. Since the pore radius $R_b$ is known from Step 1, the force constants **B** and **D** can be immediately calculated for Solutes III to VII. Quantities **B** and **D** so obtained using two CA-398 membranes were independent of $R_b$ and the result is listed in Table 3. The same procedure was applied to PPPH 8273 membranes. For Solute I, which is strongly dissociated in water, the electrostatic force represented by Eq. (2) must contribute primarily to the interaction force and, therefore, the set of

TABLE 3

Some Physicochemical Constants and Force Constants of Solutes

| | | | CA-398 | | PPPH 8273 | |
|---|---|---|---|---|---|---|
| Solute number | Solute diffusivity[a] $\times 10^9$ ($m^2/s$) | Stokes' law[b] radius $\times 10^{10}$ (m) | $\mathbf{D} \times 10^{10}$ (m) | $\mathbf{B} \times 10^{30}$ ($m^3$) | $\mathbf{D} \times 10^{10}$ (m) | $\mathbf{B} \times 10^{30}$ ($m^3$) |
| I | 0.654 | 3.73 | 2.70 | 1.73[c] | 2.20 | 1.22[c] |
| II | 0.654 | 3.73 | — | — | — | — |
| III | 0.693 | 3.52 | 2.93 | 67.9 | 1.84 | −85.9 |
| IV | 0.693 | 3.52 | 3.30 | 141 | 1.85 | −33.8 |
| V | 0.678 | 3.59 | 3.13 | 81.9 | 1.75 | −85.9 |
| VI | 0.665 | 3.66 | 3.67 | 195 | 2.87 | 69.1 |
| VII | 0.687 | 3.55 | 6.00 | 145.00 | 3.75 | 294 |

[a] Calculated by using the Wilke-Chang equation (*16*).

[b] Calculated by using solute diffusivity.

[c] $\mathbf{A} \times 10^{10}$, m.

force constants **A** and **D** were obtained for this solute. The result is also listed in Table 3.

When the force constants listed in Table 3 are combined with the pore radius listed in Table 1, we are able to calculate the solute separation data at different operating pressures. The separation data so calculated are compared with the experimental data in Fig. 1. The agreement of the calculated and experimental values is within the range of experimental error. If the model and parameters used are inadequate, the agreement shown in Fig. 1 cannot be expected.

It seems worth noting that the separation decrease with the increase in operating pressure was theoretically predicted only for Solute VII with respect to CA-398 membranes and the experiment confirmed the prediction for such systems. An exactly identical experimental result was obtained in the previous work (*3*). This is due to the very strong attractive interaction force between Solute VII and CA-398 material and the relatively large size of the pore existing in the membrane cellulose acetate material (*15*). Although there are other cases where the solute is preferentially adsorbed to the polymer material (all radical solutes with respect to CA-398 material and radical Solute VI and nonionized Solute VII with respect to PPPH 8273 material), the solute separation increases with the increase in the operating pressure, since the strong attraction is compensated for by the steric hindrance effect.

Some remarks on the force constants **B** and **D** in Table 3 are in order. As listed in Table 3, the Stokes' law radius ($r_A$) of the solutes studied ranges

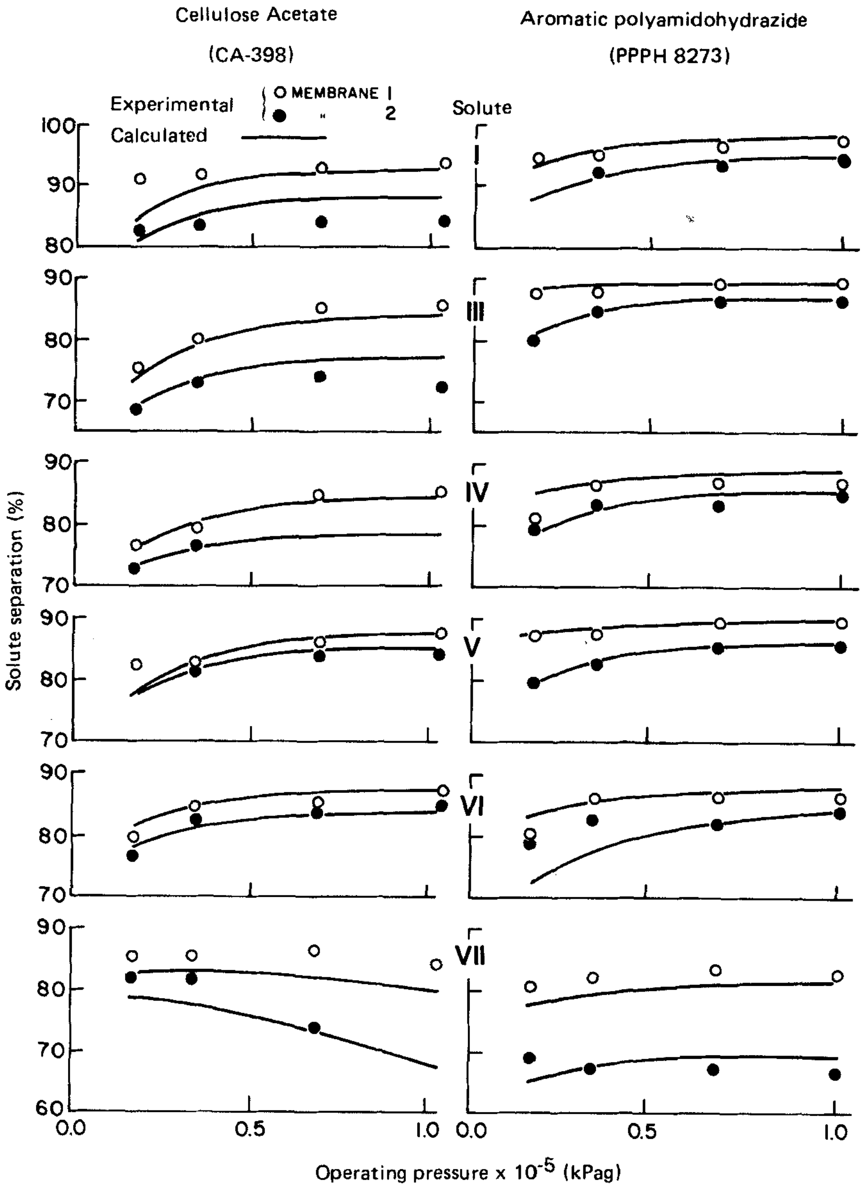

FIG. 1. Solute separation versus operating pressure. Solute concentration, $0.001 \times 10^3$ mol/m$^3$; feed flow rate, $400 \times 10^{-6}$ m$^3$/min.

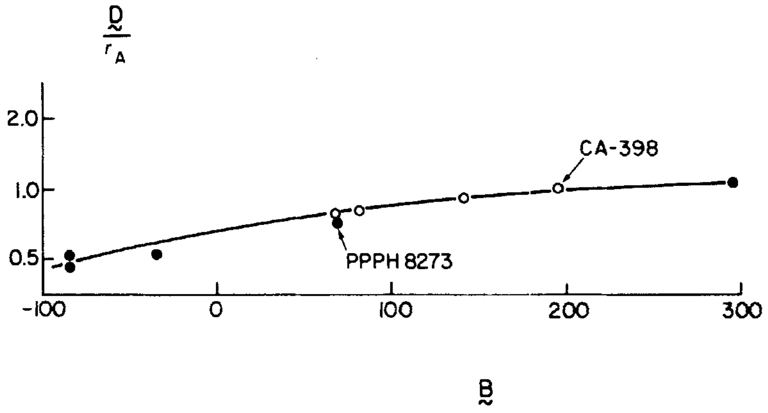

FIG. 2. $\mathbf{D}/r_A$ versus **B**. $r_A$ = Stokes' law radius of solute molecule.

from 3.55 to $3.73 \times 10^{-10}$ m. Compared with the Stokes' law radius, the quantities **D** calculated are smaller except for Solutes VI and VII for CA-398 material and Solute VII for PPPH 8273 material. Moreover, when (**D**/Stokes' law radius) is plotted versus **B** as illustrated in Fig. 2, we find there is a unique relationship between these quantities, i.e., the above ratio increases with an increase in **B**. Considering a larger (**D**/Stokes' law radius) ratio indicates more frictional force on the solute molecule due to steric factor. Figure 2 implies that such a frictional force increases when the attractive interaction between the solute and the membrane material increases.

Comparison of $R_b$ and **D** values listed in Tables 1 and 3, respectively, indicates that the size of the solutes under study is far below the size of the pore on the membrane surface. Therefore, the separation of the solute does not take place by a sieving mechanism.

## CONCLUSION

It is concluded from this work that:

(1) The radical structure affects the adsorption property of a solute with a similar hydrocarbon backbone.

(2) The adsorption property of radical solutes is further affected by the chemical structure of the polymer materials on which they are adsorbed.

(3) When the frictional forces working on a solute molecule are nearly equal, solute separation is primarily determined by the interaction force working between the solute and the polymer material.

Since the membrane transport of a radical solute is of biomedical significance, further research on this subject is called for to meet the specific needs of the application involved.

Issued as N.R.C. No. 22735.

## REFERENCES

1. D. J. Carlsson, K. H. Chan, and D. M. Wiles, in *Photodegradation and Photostabilization of Coatings* (S. P. Pappas and F. H. Winslow, eds.), ACS Symposium Series 151, 1981, p. 51.
2. E. G. Rozantsev, *Free Nitroxyl Radicals,* Plenum, New York, 1970.
3. K. Chan, T. Matsuura, and S. Sourirajan, *Sep. Sci. Technol., 18,* 223 (1983).
4. T. Matsuura, P. Blais, and S. Sourirajan, *J. Appl. Polym. Sci., 20,* 1515 (1976).
5. L. Pageau and S. Sourirajan, *Ibid., 16,* 3185 (1972).
6. T. Matsuura, P. Blais, L. Pageau, and S. Sourirajan, *Ind. Eng. Chem., Process Des. Dev., 16,* 510 (1977).
7. S. Sourirajan, *Reverse Osmosis,* Academic, New York, 1970, Chap. 3.
8. N. A. Chuduk, Yu. A. Eltekov, and A. V. Kiselev, *J. Colloid Interface Sci., 84,* 149 (1981).
9. T. Matsuura, Y. Taketani, and S. Sourirajan, *Desalination, 38,* 319 (1981).
10. T. Matsuura and S. Sourirajan, *J. Appl. Polym. Sci., 15,* 2905 (1971).
11. J. M. Dickson, T. Matsuura, P. Blais, and S. Sourirajan, *Ibid., 19,* 801 (1975).
12. T. Liu, T. Matsuura, and S. Sourirajan, *Ind. Eng. Chem., Process Des. Dev., 22,* 77 (1983).
13. T. Matsuura and S. Sourirajan, *Ibid., 20,* 273 (1981).
14. T. Matsuura, Y. Taketani, and S. Sourirajan, in *Synthetic Membranes,* Vol. II (A. F. Turbak, ed.), ACS Symposium Series 154, 1981, p. 315.
15. T. Matsuura, T. A. Tweddle, and S. Sourirajan, *Predictability of Performance of Reverse Osmosis Membranes from Data on Surface Force Parameters,* Paper Presented at the Symposium on Membrane Processes for Industrial Wastewater Treatment in the Summer National AIChE Meeting, August 29–September 1, 1982, Cleveland, Ohio.
16. C. R. Wilke and P. Chang, *AIChE J., 1,* 264 (1955).

*Received by editor March 21, 1983*